Progress In Electromagnetics Research C, Vol. 20, 43–53, 2011

ARBITRARY VOXEL SELECTION FOR ACCELERATING A RAY TRACING-BASED FIELD PREDICTION MODEL IN URBAN ENVIRONMENTS

P. Usai, A. Corucci, S. Genovesi, and A. Monorchio

Department of Information Engineering
University of Pisa, Via G. Caruso 16, Pisa I-56122, Italy

Abstract—Great accuracy and reasonable computational time are desirable in a deterministic ray tracing model for an efficient radio frequency planning. An algorithm to speed up a ray tracing engine is described which allows to select arbitrary areas around transmitters and receivers by dividing the scene in a voxel chessboard. The reliability of the algorithm has been evaluated by comparing measured and predicted path losses in real urban scenarios while the algorithm performance is expressed in terms of computational time reduction.

1. INTRODUCTION

The goal of propagation modeling is to describe with a mathematical formulation the spreading of electromagnetic waves inside the considered scenario. Many empirical, statistical and physical models are used for this purpose. Among the asymptotic methods, inverse 3D deterministic Ray Tracing (RT) models are characterized by an accurate prediction of the electromagnetic field both in the case of an outdoor site as well as an indoor location. In Radio Frequency (RF) system planning, the RT propagation model and data of the scenario can be used to predict the RF coverage area of a transmitter (T_x). This analysis allows to determine the received signal strength at the receiver (R_x), the Path Loss (PL) of a wireless link and channel impairment such as delay spread due to multi-path fading. The knowledge of these parameters before the wireless system setting-up leads to an installation cost reduction together with a quality of services increase. For example, it is possible to estimate the minimum number of antennas and their best locations in order to guarantee a

Received 4 January 2011, Accepted 23 February 2011, Scheduled 27 February 2011
Corresponding author: Simone Genovesi (simone.genovesi@iet.unipi.it).

suitable RF coverage of an area. Then, the *'in situ'* measurements can be carried out as an *'a posteriori'* check for validate the predicted results. Moreover, the level of the electromagnetic radiation can be accurately predicted in order to investigate possible health hazards or to test the fulfillment of the limits of exposition defined in norms and recommendations.

In the RT approach, buildings and terrain are geometrically modeled by means of polygonal plane facets. The time required by the RT algorithm to compute all rays connecting T_xs and R_xs exponentially rises as the number of facets linearly increases [1]. Therefore the physical coherence of the deterministic approach leads to a boost of the computational time and this propagation model is thus often considered time expensive if compared to the empirical and statistical ones.

In order to reduce the computational time and the memory requirement, many solutions have been proposed over the last decades, also in the field of visualization applications. When the RT is based on an inverse algorithm, the visibility conditions between each couple of facets play an important role in the computation time reduction since it minimizes the number of times the visibility test routines are applied. For this reason many techniques addressing this aspect are based on the visibility conditions optimization. They split the space seen from a point in angular or axis-aligned regions and store the facets of the model in the regions where they belong. For example, Angular Z-Buffer (AZB), Space Volumetric Partitioning (SVP), Occluder Fusion, and Binary Space Partitioning (BSP), have received great attention [1–3]. Because they act only by speeding up geometrical checks, they do not introduce any approximation in the field prediction compared with the full 3D RT analysis. Another approach is the hybrid imaging technique [4], where the 3D paths research starts from 2D image generations in horizontal and vertical planes. Another method [5] combines horizontal 2D RT and knife-edge diffraction model to take into account the street canyon effect and the radio propagation above rooftop. In [6], a method based on a data base preprocessing is presented. The facets and edges are divided into tiles and segments and the possible rays between them are computed and stored in a file. When the scene database remains the same and the T_x moves into the scene, this method shows its best results, since the data stored in the file prevents to analyze again the scenario. A 2D model that simplifies the real scenario by considering only the horizontal 2D propagation mode between infinitely tall buildings is described in [7]. Recently, it has been proposed a simplification based on a heuristic preprocessing of the scenario database [8]. This technique, given the T_x and R_x

positions, identifies the active part of the scene database selecting all buildings located within an ellipse of focuses T_x and R_x, and in line of sight with the T_x and/or R_x. However, when the distance between T_x and R_x and the largest scene dimension are comparable in order of magnitude, the ellipse surface almost overlies the whole scenario and the method becomes inefficient. To overcome this drawback due to an intrinsic geometric limit, we propose a pre-processing refinement of the scene characterized by a higher degree of flexibility of the selected area that will be subsequently analysed by the RT method. By using a grid space division, a minimum area, based on the line connecting T_x and R_x, is selected and it can also be refined or modified by the user.

Our approach has been implemented on a ray tracer [3] which employs an inverse 3D deterministic RT algorithm, based on the image method, to simulate the electromagnetic propagation in complex environments. Fixed k as the order of simulation, the code engine is able to find all rays formed by sequences of up to k elementary contributions including reflections and diffractions. A particular emphasis will be given to the employment of our strategy for propagation in urban scenarios since it is of paramount importance in the research field and in many applications such as localization schemes [9], channel modeling [10, 11], electromagnetic mapping in urban areas [12–15]

2. ALGORITHM DESCRIPTION

In the first step a bounding box containing all the buildings in the scene is defined and then a uniform adaptive grid [16] is locally applied. As shown in Fig. 1, the space is divided into a set of N_v cells called voxels, an abbreviation of *elemental volumes* in analogy to pixels (*picture elements*).

The number of voxels N_v is estimated by

$$N_v = \left\lceil \frac{Dim_x \cdot Dim_y}{Dist_x \cdot Dist_y} \right\rceil \tag{1}$$

where Dim_x and Dim_y are the grid dimensions along X and Y axes. The distance between T_x and R_x along the X axis is $Dist_x$ while the distance along Y axis is $Dist_y$ (Fig. 2).

The total number of voxels N_v is set to be within the interval $[30, 400]$ in order to have a useful partitioning of the scenario.

A higher number of voxels would make cumbersome the arbitrary selection operated by the user and would create voxels which are too small and hence useless. Moreover, this upper bound of the interval is useful when the distance between T_x and R_x is smaller than the

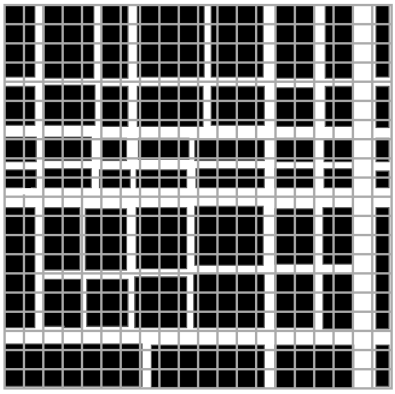

Figure 1. The uniform grid divides into voxels the considered scenario.

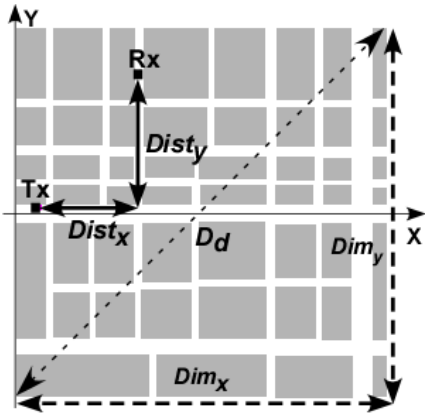

Figure 2. Visualization of the parameters for a scenario with a given couple of T_x and R_x.

diagonal D_d of the scenario since it allows a finer voxel discretization of the investigated area. The lower bound is necessary to manage the case when the distance between T_x and R_x and the diagonal D_d are comparable. If N_v in (1) is less or more than the lower or the upper bound respectively, its value is set equal to the nearest bound. If T_x and R_x are aligned along a reference axis, the value of N_v is set equal to the upper bound.

Because the chosen voxel's footprint is the square shape, the number of subdivisions along X and Y, N_x and N_y, are taken proportionally to the grid dimensions along X and Y axes. Given the proportional factors

$$\begin{array}{ll} \beta = \frac{Dim_x}{Dim_y}, & Dim_x > Dim_y \\ \gamma = \frac{Dim_y}{Dim_x}, & Dim_x < Dim_y \end{array} \tag{2}$$

we obtain

$$N_v = N_x \cdot N_y = \begin{cases} \beta \cdot N_y \cdot N_y = \beta \cdot N_y^2 & Dim_x > Dim_y \\ \gamma \cdot N_x \cdot N_x = \gamma \cdot N_x^2 & Dim_x < Dim_y \end{cases} \tag{3}$$

and

$$\begin{array}{lll} N_y = \sqrt{\frac{N_v}{\beta}}, & N_x = \beta \cdot N_y, & Dim_x > Dim_y \\ N_x = \sqrt{\frac{N_v}{\gamma}}, & N_y = \gamma \cdot N_x, & Dim_x < Dim_y \end{array} . \tag{4}$$

If more than one R_x is present, the algorithm is applied on the nearest one to the T_x. By means of a matrix structure the membership

of facets to the voxel is stored. By using a grid space division, the default voxel selection is defined by the union of all voxels crossed by the straight lines linking the T_x and each R_x. Next, a further subset of cells can be excluded by the user who refines or modifies the set of voxels considered. Finally, it is important to underline that the RT engine will only search the rays which interact with facets contained in the selected voxels.

3. THE ALGORITHM VALIDATION FOR A TEST-CASE URBAN SCENARIO

The accuracy of the algorithm is tested by analyzing the scene shown in Fig. 3. The scenario represents a 1.5 GHz communication microcell in a Tokyo street grid [17] where a line of receivers R_{xi} is placed along the path CAD. The model of the buildings uses a relative permittivity ε_r equal to 15 and a conductivity σ of 7 S/m. The T_x antenna is a half-lambda dipole and the R_{xi} antennas are assumed omnidirectional. The grid sizes and the evaluated number of rows and columns are summarized in Table 1, where *Minimum Dist* stands for the $Dist_x$ and $Dist_y$ parameters relative to the nearest R_x to the T_x. In order to show the flexibility and reliability of the proposed approach, two different areas are considered for the analysis. The former (case 1) is enclosed by a continuous gray line in Fig. 3(a) and represents the default voxels selection of the algorithm. The latter is highlighted in grey in Fig. 3(b) (case 2) and represents an arbitrary finer selection

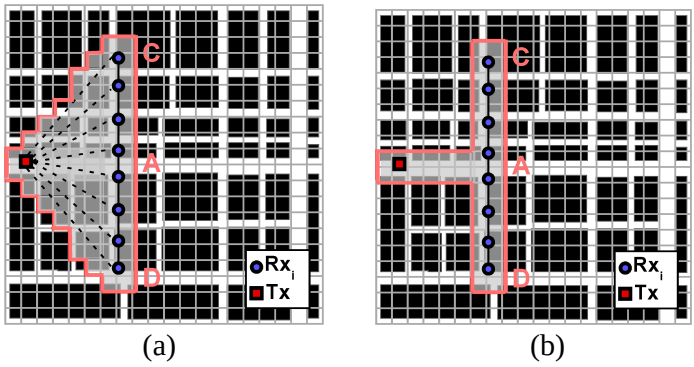

Figure 3. Voxel partitioning of the Tokyo's scenario with two different selected areas: (a) Case 1 with default voxel selection by using the line of connection among T_x and R_{xi}; (b) case 2 with refinement performed by the user.

Table 1. Tokyo's scenario geometry.

	Along X	**Along Y**
Dim[m]	800	800
Minimum Dist[m]	218	0
Number of Subdivisions [N_x, N_y]	20	20
Total number of Voxels	400	
Number of Selected Voxels (case 1)	78	
Number of Selected Voxels (case 2)	44	

Table 2. Ray tracing time vs order of simulation in Tokyo's scenario.

k	**Full RT**	**Prediction 1**	**Gain 1 %**	**Prediction 2**	**Gain 2 %**
I	0 h,0m,31 s	0 h,0 m,0.2 s	99.3	0 h,0 m,0.2 s	99.3
II	0 h,1 m,0 s	0 h,0 m,1.5 s	97.5	0 h,0 m,1.4 s	97.6
III	0 h,5 m,35 s	0 h,0 m,10.5 s	96.9	0 h,0 m,6.5 s	98.1
IV	2 h,13 m,24 s	0 h,3 m,21 s	97.5	0 h,1 m,22 s	99.0
V	111 h,0 m,0 s	1 h,27 m,44 s	98.7	0 h,26 m,12 s	99.6

operated by the user. This arbitrary selection can be performed in an urban scenario by considering the regular geometry of the buildings in the default selected area. This simple observation can provide the user a method to individuate the canyon-like propagation and thus the suitable finer voxel selection. It is shown that no relevant contributions are lost using both the two different areas as opposed to the Full RT estimation but it is also worthwhile to mention that even the default selection will guarantee great advantages with respect to the simulation of the overall area as reported in the following.

The measured data refer to the PL fluctuation along the line CAD and are taken from [17].

The analysis has been run with an order of simulation $k = 5$ for both case 1 and 2. A Full RT analysis of the scene with the same order of simulation has been run too. A satisfactory comparison of predicted and measured PL is shown in Fig. 4 and Fig. 5 and proves the accuracy of the estimate which is able to estimate level of PL as low as -120 dB. Moreover it shows that no relevant contributions are lost using both the two different areas as opposed to the Full RT estimation. The improvements in terms of RT Time reduction are summed up in Table 2 for both case 1 and 2.

It is important to underline that a smart selection of the analyzed area can further improve the acceleration as proven by the fact that

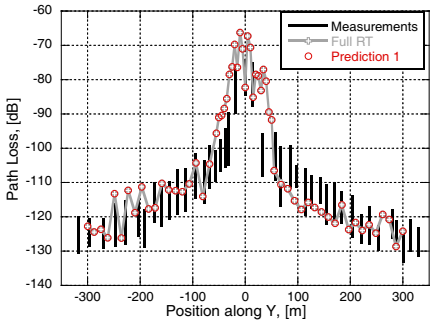

Figure 4. Comparison of the Path Loss estimations by the Full RT analysis and the proposed algorithm.

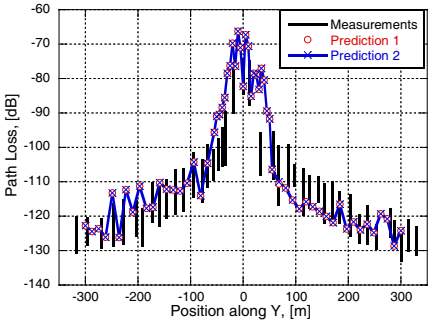

Figure 5. Comparison of the Path Loss estimations by two different applications of the proposed algorithm.

the same PL prediction has been obtained in both cases 1 and 2 but with a RT Time (RTT) reduction of about 70% in the latter case where only 44 voxels are considered instead of 78.

4. THE ALGORITHM PERFORMANCE EVALUATION

The city of Lucca in Tuscany (Italy) is to the scenario used to evaluate the computational time saving obtained by employing the proposed algorithm. In Fig. 6, the overall city map with the T_x and R_xs locations and the voxel partitioning are shown while the main characteristics of the scenario's settings are reported in Table 3. By recurring to inspection suggested in the previous section we notice the ancient city of Lucca is characterized by high buildings and narrow and winding streets. In the considered configuration, the T_x and

Table 3. Lucca's scenario geometry.

	Along X	**Along** Y
Dim [m]	1718	1264
Minimum Dist [m]	82	250
# Subdivisions [Nx, Ny]	21	10
# Voxels	210	
# Selected Voxels	5	
Number of Tx	1	
Number of Rx	1	

Table 4. Evaluation of the map reduction in terms of covered area and number of facets and edges.

Target	Total Map	Reduced Map	Gain %
Area [km^2]	2.17	0.051	97.6
#Facets	7800	234	97
#Edges	8511	329	96

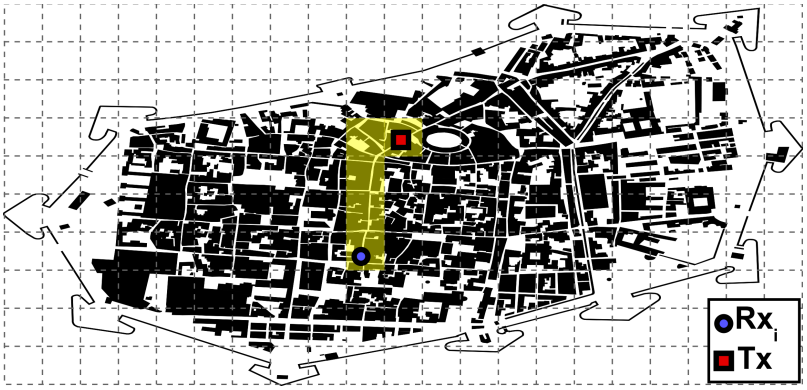

Figure 6. View of the city of Lucca, Italy where the selected voxels are highlighted.

R_x are under the roof level thus, the main propagation mechanisms involved in this street canyon analysis are reflections between high planes (opposite building fronts). The voxels selected by the user to cover the street canyon linking T_x and R_x are highlighted while the size and number of subdivisions are resumed in Table 3. An evaluation of the computational cost reduction provided by the application of the algorithm is summarized in Table 4. As a result, the RT engine has to process only the 3% of all facets and the 4% of all edges. In order to evaluate the impact of the accelerating technique with respect to the order of elementary contributes taken into account, for the same map and T_x and R_x locations, the order of simulation has been increased from 1 to 6.

The evaluation of ray propagation in the selected area is reported in Fig. 7 for a simulation order equal to 6. The performance of the speed-up method in terms of saved RT time, that is to say the running RT solver time, is summarized in Fig. 8 where the percentage of saved time with respect to the full ray tracing method is reported as a function of the simulation order considered. All the simulation

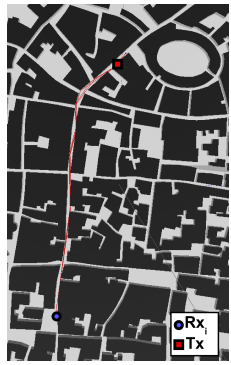

Figure 7. Ray propagation between the transmitter and the receiver for simulation order equal to 6.

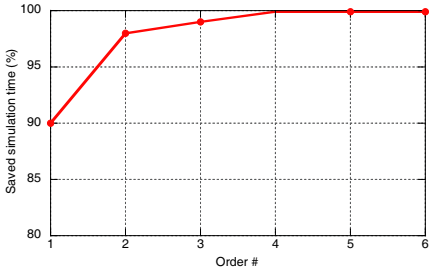

Figure 8. Percentage of saved time as a function of the simulation order.

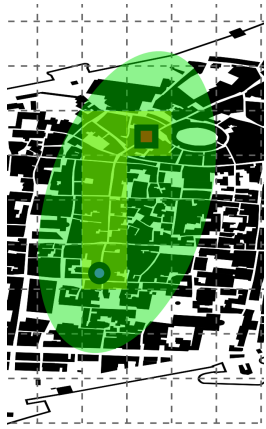

Figure 9. Zoom on the selected voxels in Lucca's scenario.

has been performed by an Intel Core 2 CPU X6800, with 2 GB of RAM. The proposed method provides a robust reduction of the area considered for the RT (less than 2% of the total) and, as a consequence, the RTT dramatically decreases. In order to highlight the flexibility and efficiency of this approach it is worthwhile to highlight that in this case the selected area were elliptic, the number of considered facets would have been much higher as apparent from Fig. 9. Moreover, the gain in terms of computational time saving is more and more evident with high order of simulation.

5. CONCLUSION

An arbitrary and flexible shape selection of the investigated area for a RT analysis has been proposed. The method is particularly suitable for evaluating propagation in urban scenarios where not all the objects are involved in the ray propagation between the transmitter and the receiver. There is no restriction to canonical shapes such as circles or ellipses for the selection of the area under test since the partitioning into voxel provides the user to define irregular polygons thus avoiding to include unnecessary elements. The accuracy of the method and its performances in terms of RTT have been proved by using comparison between simulations and measurements. It has also been shown that the algorithm allows to consider high simulation orders in a considerable shorter RTT with respect to a full RT analysis.

REFERENCES

1. Catedra, M. F., J. Perez, F. S. de Adana, and O. Gutierrez, "Efficient ray-tracing techniques for three-dimensional analyses of propagation in mobile communications: Application to picocell and microcell scenarios," *IEEE Antennas and Prop. Mag.*, Vol. 40, No. 2, 15–28, Apr. 1998.
2. Bittner, J., P. Wonka, and M. Wimmer, "Visibility preprocessing for urban scenes using line space partitioning," *IEEE Proceed. 9th Conf. Computer Graphics and Applications*, 276–284, Oct. 2001.
3. Santini, S., S. Bertini, and A. Monorchio, "An acceleration technique for ray tracing simulation based on a shadow volumetric binary and line space partitioning," *IEEE Proceed. Antennas and Propag.*, 1–4, Jul. 2008.
4. Athanasiadou, G. E. and A. R. Nix, "A novel 3-D indoor ray-tracing propagation model: The path generator and evaluation of narrow-band and wide-band predictions," *IEEE Trans. Vehicular Technology*, Vol. 49, No. 4, 1152–1168, Jul. 2000.
5. Corre, Y., Y. Lostanlen, and Y. Le Helloco, "A new approach for radio propagation modeling in urban environment: Knife-edge diffraction combined with 2D ray-tracing," *IEEE Proceed. 55th Vehicular Tech. Conf.*, Vol. 1, 507–511, 2002.
6. Rautiainen, T., R. Hoppe, and G. Wölfle, "Measurements and 3D Ray Tracing propagation predictions of channel characteristics in indoor environments," *IEEE 18th Intern. Symp. PIMRC*, 1–5, Sep. 2007.
7. Rizk, K., J. F. Wagen, and F. Gardiol, "Two-dimensional

ray-tracing modeling for propagation prediction in microcellular environments," *IEEE Trans. Vehicular Technology*, Vol. 46, No. 2, 508–518, May 1997.

8. Degli Espositi, V., F. Fuschini, E. M. Vitucci, and G. Falciasecca, "Speed-up techniques for Ray Tracing field prediction models," *IEEE Trans. Antennas and Propag.*, Vol. 57, No. 5, 1469–1480, May 2009,
9. Song, H. B., H. G. Wang, K. Hong, and L. Wang, "A novel source localization scheme based on unitary esprit and city electronic maps in urban environments," *Progress In Electromagnetics Research*, Vol. 94, 243–262, 2009.
10. El-Sallabi, H. M. and P. Vainikainen, "Radio wave propagation in perpendicular streets of urban street grid for microcellular communications. Part I: Channel modeling-abstract," *Progress In Electromagnetics Research*, Vol. 40, 229–254, 2003.
11. Fugen, T., J. Maurer, T. Kayser, and W. Wiesbeck "Capability of 3-D ray tracing for defining parameter sets for the specification of future mobile communications systems" *IEEE Trans. Antennas and Propag.*, Vol. 54, No. 11, 3125–3137, Nov. 2006.
12. Giliberti, C., F. Boella, A. Bedini, R. Palomba, and L. Giuliani, "Electromagnetic mapping of urban areas: The example of monselice (Italy)," *PIERS Online*, Vol. 5, No. 1, 2009.
13. Di Giampaolo, E. and F. Bardati, "A projective approach to electromagnetic propagation in complex environments," *Progress In Electromagnetics Research B*, Vol. 13, 357–383, 2009.
14. Liang, G. and H. L. Bertoni, "A new approach to 3-D ray tracing for propagation prediction in cities," *IEEE Trans. Antennas and Propag.*, Vol. 46, No. 6, 853–863, Jun. 1998.
15. Yun, Z., Z. Zhang, and M. F. Iskander, "A ray-tracing method based on the triangular grid approach and application to propagation prediction in urban environments," *IEEE Trans. Antennas and Propag.*, Vol. 50, No. 5, 750–758, May 2002.
16. Klimaszewski, K. S. and T. W. Sederberg, "Faster ray tracing using adaptive grids," *IEEE Computer Graphics and Applications*, Vol. 17, No. 1, 42–51, Jan.–Feb. 1997.
17. Tan, S. Y. and H. S. Tan, "Microcellular communications propagation model for a city street grid," *IEEE Proceed. Antennas and Propag.*, Vol. 3, 1910–1913, Jun. 1994.